

# Unexpected NADPH Hydratase Activity in the Nitrile Reductase QueF from *Escherichia coli*

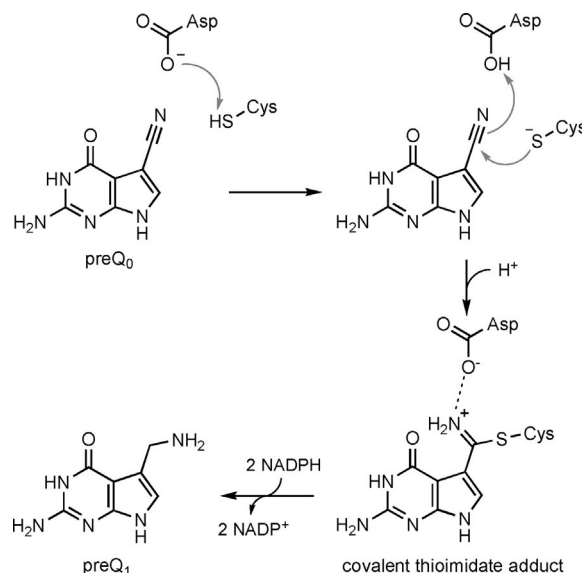
Jihye Jung,<sup>[a, b]</sup> Jan Braun,<sup>[a]</sup> Tibor Czabany,<sup>[a, b]</sup> and Bernd Nidetzky\*<sup>[a, b]</sup>

The nitrile reductase QueF catalyzes NADPH-dependent reduction of the nitrile group of preQ<sub>0</sub> (7-cyano-7-deazaguanine) into the primary amine of preQ<sub>1</sub> (7-aminomethyl-7-deazaguanine), a biologically unique reaction important in bacterial nucleoside biosynthesis. Here we have discovered that the QueF from *Escherichia coli*—its D197A and E89L variants in particular (apparent  $k_{\text{cat}} \approx 10^{-2} \text{ min}^{-1}$ )—also catalyze the slow hydration of the C5=C6 double bond of the dihydronicotinamide moiety of NADPH. The enzymatically C6-hydrated NADPH is a 3.5:1 mixture of *R* and *S* forms and rearranges spontaneously

through anomeric epimerization ( $\beta \rightarrow \alpha$ ) and cyclization at the tetrahydronicotinamide C6 and the ribosyl O2. NADH and 1-methyl- or 1-benzyl-1,4-dihydronicotinamide are not substrates of the enzymatic hydration. Mutagenesis results support a QueF hydratase mechanism, in which Cys190—the essential catalytic nucleophile for nitrile reduction—acts as the general acid for protonation at the dihydronicotinamide C5 of NADPH. Thus, the NADPH hydration in the presence of QueF bears mechanistic resemblance to the C=C double bond hydration in natural hydratases.

The enzyme QueF is a nitrile reductase that catalyzes NADPH-dependent reduction of a nitrile group into a primary amine.<sup>[1–3]</sup> The enzyme's natural reaction is conversion of 7-cyano-7-deazaguanine (preQ<sub>0</sub>) into 7-aminomethyl-7-deazaguanine (preQ<sub>1</sub>)<sup>[1,4]</sup> (Scheme 1) in bacterial nucleoside (queuosine) biosynthesis.<sup>[4–7]</sup> Enzymatic four-electron reduction of a nitrile to an amine has drawn considerable attention, both because of the mechanistic challenges presented by this—apparently unique to biology—chemical transformation and because of the possible opportunities opened up by it for biocatalytic synthesis.

The proposed mechanism of QueF catalysis involves a thioimide covalent enzyme-preQ<sub>0</sub> adduct that undergoes reduction by NADPH in two catalytic steps via an imine intermediate (Scheme 1).<sup>[2,3,8–10]</sup> The QueF active site consists of a cysteine/aspartate dyad of residues that operate in a functionally interconnected manner in covalent enzyme catalysis, as shown in Scheme 1.<sup>[3,8,11,12]</sup> As part of our investigation of the QueF mechanism, we substituted the relevant Cys190 (by Ala and



**Scheme 1.** Proposed mechanism of reduction of preQ<sub>0</sub> into preQ<sub>1</sub>, catalyzed by the nitrile reductase QueF. The active-site dyad Cys and Asp act together in covalent catalysis. Reduction of the thioimide enzyme adduct occurs in two NADPH-dependent steps via an imine intermediate (not shown).

Ser) and Asp197 (by Ala and His) in the enzyme from *Escherichia coli* (ecQueF) and studied preQ<sub>0</sub> reduction in the presence of the enzyme variants.<sup>[12]</sup> For certain enzyme variants (e.g., D197A) we noted that a large amount of the NADPH consumed was not accounted for either in the preQ<sub>0</sub> converted or in the NADP<sup>+</sup> released. Enzymatic use of NADPH, uncoupled not coupled to reduction of the nitrile substrate and through a non-oxidative pathway leading to a product different from NADP<sup>+</sup>, was the starting point of the current study, examining the mechanistic origin of an apparently unbalanced reaction.

The nicotinamide coenzymes NADH and NADPH are unstable compounds prone to spontaneous<sup>[13–16]</sup> and enzyme-promoted degradation.<sup>[17,18]</sup> Coenzyme stability is of considerable

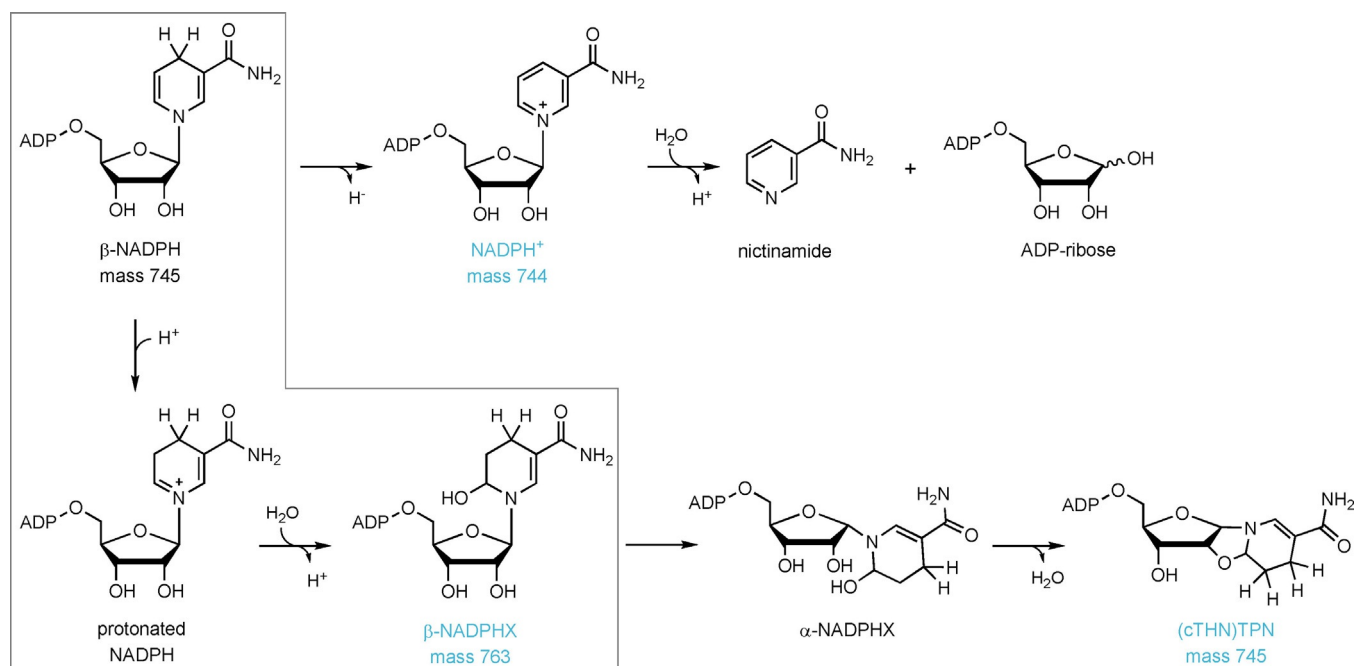
[a] Dr. J. Jung, J. Braun, Dr. T. Czabany, Prof. Dr. B. Nidetzky  
Institute of Biotechnology and Biochemical Engineering  
Graz University of Technology, NAWI Graz  
Petersgasse 10/12, 8010 Graz (Austria)  
E-mail: bernd.nidetzky@tugraz.at

[b] Dr. J. Jung, Dr. T. Czabany, Prof. Dr. B. Nidetzky  
Austrian Centre of Industrial Biotechnology  
Petersgasse 14, 8010 Graz (Austria)

Supporting information and the ORCID identification numbers for the authors of this article can be found under <https://doi.org/10.1002/cbic.201900679>.

© 2019 The Authors. Published by Wiley-VCH Verlag GmbH & Co. KGaA. This is an open access article under the terms of the Creative Commons Attribution Non-Commercial License, which permits use, distribution and reproduction in any medium, provided the original work is properly cited and is not used for commercial purposes.

This article is part of a joint Special Collection dedicated to the Biotrans 2019 symposium. To view the complete collection, visit our homepage



**Scheme 2.** Reaction pathways leading to NADPH degradation in spontaneous and enzyme-promoted conversions. The uncoupled pathway (NADPH conversion not leading to  $\text{NADP}^+$ ) involves hydration of NADPH to NADPHX followed by epimerization/cyclization, leading to O $2'$ - $\beta$ -6-cyclo-1,4,5,6-tetrahydronicotinamide adenine dinucleotide phosphate [(cTHN)TPN]. The enzymatic reaction identified in this study is marked by the box. The coupled pathway (NADPH conversion leading to  $\text{NADP}^+$ ) entails formation of  $\text{NADP}^+$  through known oxidation reactions of NADPH: when O $_2$  is present, for example.

practical importance in biocatalytic<sup>[19,20]</sup> and analytical applications.<sup>[21]</sup> It also has high relevance for in vivo biology.<sup>[22]</sup> Understanding the mechanisms leading to NAD(P)H degradation is fundamentally important and might become useful in informing strategies for stabilization.

The  $\text{NAD(P)}^+$  formed by oxidation can be hydrolyzed at basic pH ( $\geq 7.5$ ),<sup>[23]</sup> as shown in Scheme 2. At low pH ( $\leq 6.8$ ), NADH and NADPH can become hydrated at the C5=C6 double bond of the dihydronicotinamide ring (Scheme 2).<sup>[15,16,24–26]</sup> The hydrated form, often referred to as NADHX or NADPHX, reacts further through anomeric epimerization and cyclization at the nicotinamide C6 and the ribosyl O2 (Scheme 2).<sup>[16,24]</sup> Taken together, the hydrated and cyclized forms are also known as the “acid-modified” products of NADH<sup>[16,24]</sup> and NADPH.<sup>[15,25]</sup> Glycer-aldehyde 3-phosphate dehydrogenase (GAPDH) catalyzes the conversion of NADH to NADHX,<sup>[18,27,28]</sup> but no analogous enzymatic transformation of NADPH has yet been reported. Discovery of an enzymatic equivalent of the acid-catalyzed degradation of NADPH might have biological significance.<sup>[29–35]</sup> Knowing the enzymes other than GAPDH that could play a role in the formation of NAD(P)HX is therefore important. In addition, acid-modified products of NAD(P)H are potent inhibitors of several dehydrogenases.<sup>[25,36]</sup>

We show here that ecQueF—its single-site variants D197A and E89L in particular—catalyzes (at a slow rate) the degradation of NADPH in the absence of the nitrile substrate preQ $_0$ . We identify the enzymatically formed degradation product as  $\beta$ -6-hydroxy-1,4,5,6-tetrahydronicotinamide adenine dinucleotide phosphate (NADPHX, Scheme 2). We also show that NADPHX rearranges spontaneously into the corresponding cy-

clized product. We demonstrate that the enzymatic hydration of NADPH is slightly stereoselective, yielding about 3.5-fold higher amounts of (*R*)-NADPHX than of (*S*)-NADPHX. On the basis of results of mutagenesis, we suggest an NADPH hydratase mechanism for ecQueF. This mechanism involves the catalytic nucleophile (Cys190) of the canonical nitrile reduction as the general acid for protonation at the 1,4-dihydronicotinamide C5 atom. We further show that coenzyme hydration is specific for NADPH whereas NADH and 1-methyl- or 1-benzyl-1,4-dihydronicotinamide are not accepted as substrates. We point out mechanistic analogies between the “moonlighting” hydratase activity of ecQueF and C=C double bond hydration by natural hydratases.

## Results and Discussion

### Discovery of NADPH hydration activity of ecQueF enzymes

Single-site variants of ecQueF (C190A, C190S, D197A, D197H) were isolated and characterized for activity in preQ $_0$  reduction, along with the wild-type enzyme.<sup>[12]</sup> Catalytic reactions of the variants with preQ $_0$  were peculiar in that their NADPH consumption greatly exceeded the corresponding preQ $_1$  release, and the excess utilization of NADPH was largely uncoupled from the formation of  $\text{NADP}^+$ . The wild-type enzyme used the NADPH for preQ $_0$  reduction under these conditions (Table S1 in the Supporting Information). In the following text we refer to coupled and uncoupled reactions of NADPH, leading to  $\text{NADP}^+$  and to products other than  $\text{NADP}^+$ , respectively.

The D197A variant displayed the feature of the uncoupled reaction with NADPH in particular, as shown in Table S1. Being unusual among dehydrogenases/reductases, the uncoupled utilization of NADPH drew our immediate interest and was therefore analyzed in detail. HPLC absorbance traces revealed two prominent peaks (Figure S1), the abundance of which in reaction samples was correlated with the uncoupled NADPH conversion. We performed experiments in the absence of preQ<sub>0</sub> and showed that the uncoupled conversion of NADPH proceeded readily under these conditions (Table 1). Interesting-

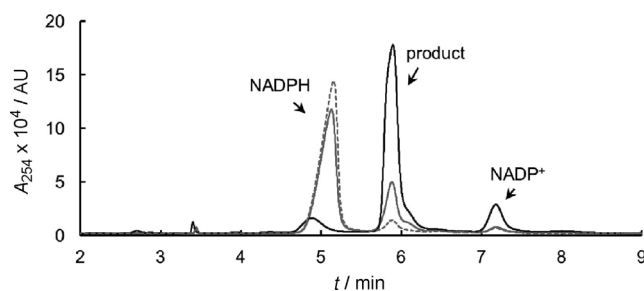


**Figure 1.** HPLC analysis of degradation of NADPH in the presence of the D197A variant of ecQueF. Rearrangement of NADPH (500 μM) in the presence of the D197A variant (50 μM, black) and spontaneous reaction (gray) were analyzed after incubation at 25 °C for 26 h. The NADPH solution at the start of the reaction is shown by a gray dashed line. Mass analysis shows that the product peak consisted of a 745 mass as well as a 763 mass species. The mass intensity ratio for the two species changed depending on the conditions used in the reaction and in the analysis procedure.

**Table 1.** Reaction rates at pH 7.5 associated with NADPH degradation in the presence of wild-type ecQueF and variants thereof. The rates are expressed in terms of product released (or substrate converted). Reactions were carried out in Tris buffer (100 mM, pH 7.5; 50 mM KCl; 1.15 mM TCEP) and used 500 μM NADPH. The standard deviations shown are from triplicate measurements.

	NADPH	Reaction rate [ $\mu\text{mol L}^{-1} \text{min}^{-1}$ ]		A340 <sup>[d]</sup>
		NADP <sup>+</sup>	NADPHX <sup>[a]</sup>	
no enzyme	0.08 ± 0.01 (0.08 ± 0.01 <sup>[c]</sup> )	0.001 ± 0.0002 (0.036 ± 0.001 <sup>[c]</sup> )	0.05 ± 0.01 (0.037 ± 0.001 <sup>[c]</sup> )	0.07 ± 0.01 (0.09 ± 0.01 <sup>[c]</sup> , 6.45 <sup>[e]</sup> )
wild type <sup>[b]</sup>	0.18 ± 0.01	0.062 ± 0.011	0.11 ± 0.014	n.m.
C190A <sup>[b]</sup>	0.06 ± 0.01	0.038 ± 0.002	0.03 ± 0.006	n.m.
C190S <sup>[b]</sup>	0.08 ± 0.01	0.036 ± 0.011	0.03 ± 0.008	n.m.
D197A <sup>[b]</sup>	0.71 ± 0.07 (0.50 ± 0.05 <sup>[c]</sup> )	0.058 ± 0.006 (0.01 ± 0.002 <sup>[c]</sup> )	0.70 ± 0.07 (0.49 ± 0.05 <sup>[c]</sup> )	0.74 ± 0.07 (0.65 ± 0.05 <sup>[c]</sup> )
D197H <sup>[b]</sup>	0.19 ± 0.01	0.071 ± 0.011	0.10 ± 0.021	n.m.
E89L <sup>[b]</sup>	0.40 ± 0.04	0.089 ± 0.008	0.38 ± 0.05	0.37 ± 0.02

[a] Calculated from the product peak area (Figure 1). [b] The enzyme concentration used was 50 μM. [c] Reaction in the Tris buffer used DTT instead of TCEP. [d] Rates determined from the decrease in absorbance at 340 nm, as shown in Figure 2E. [e] Rate of the spontaneous reaction of NADPH at pH 3.5, leading to the "acid-modified" product according to ref. [37]. n.m.: not measured.

ly, in the control reaction in the absence of the enzyme, some NADPH conversion was observed as well (Figure 1). It occurred almost exclusively via the uncoupled pathway (Figure 1 and Table 1) when tris(2-carboxyethyl)phosphine (TCEP) was present. When TCEP was replaced by dithiothreitol (DTT), both the coupled and uncoupled reaction pathways contributed to NADPH degradation (Table 1). Note that TCEP, besides being a reducing agent, is a polybasic anion potentially capable of affecting the NADPH degradation,<sup>[18]</sup> whereas DTT is not.

The enzymes used (Table 1) differed in their effects on the NADPH conversion. The D197A variant accelerated the uncoupled conversion about 14-fold, relative to the control, and nearly all NADPH was degraded enzymatically by this pathway (Figure 1). Use of DTT instead of TCEP did not affect the degradation pathway utilized by the D197A variant and only marginally influenced its activity. The other variants and the wild-type enzyme hardly accelerated the overall NADPH conversion relative to the control, but caused a marked shift in the conversion pathway preferentially utilized (Table 1).

Wild-type enzyme and D197H variant catalyzed the utilization of both NADPH degradation pathways, with the uncoupled rate ( $V_{\text{NADPHX}}$  in Table 1) accounting for about 53–61% of the total NADPH degradation rate ( $V_{\text{NADPH}}$ ). As discussed later, it is mechanistically relevant that NADPH conversion in the presence of the Cys190 variants showed the strongest involvement of the coupled (oxidative) pathway to NADP<sup>+</sup> ( $V_{\text{NADP}^+}$ ), accounting for 45–63% of the total  $V_{\text{NADPH}}$  (Table 1).

Additionally, the E89L variant, in the absence of preQ<sub>0</sub>, was found to promote the uncoupled conversion of NADPH (95% strongly) (Table 1). The uncoupled reaction in the presence of the E89L variant at pH 7.5 was about 1.8 times slower than the same uncoupled reaction in the presence of the D197A variant. Note: the oxidative conversion of NADPH was affected by the presence of O<sub>2</sub> and the buffer composition (data not shown). This is a well-known reaction of NAD(P)H in solution and in the presence of enzymes, so it was not pursued here.<sup>[14,17,23]</sup>

From LC-MS analysis we identified the product of the uncoupled NADPH conversion as having the mass of NADPH hydrate (763; 1 H<sup>-</sup>, 762; 2 H<sup>-</sup>, 380.5). Additionally, we observed another species with the same mass as NADPH (745; 1 H<sup>+</sup>, 746; 1 H<sup>-</sup>, 744). This suggested that two main products had arisen from the uncoupled conversion of NADPH. In a UV/Vis spectrum, the products displayed maximum absorption at 266 nm, but unlike NADPH showed no absorption at 340 nm (Figure 2A). These mass data and spectral properties match precisely with the acid-modified products.<sup>[16,24,25]</sup> The detected product mass of 763 thus corresponds to NADPHX and the product mass of 745 to (cTHN)TPN (cyclized NADPHX), as shown in Scheme 2 and Figure 3A. As judged from the relative mass intensities in LC-MS analysis, the ratio of hydrated to cyclized product was strongly dependent upon the reaction conditions used. When TCEP was added, spontaneous or enzymatic conversion of NADPH gave a 1:3 ratio for hydrated and cyclized product. When DTT was used instead, the ratio was changed to 2:1. We also noted that slightly acidic conditions (pH 6.67) in the analysis could cause a shift in ratio toward the cyclized product. To prevent this, the analysis was always done at pH 7.5.

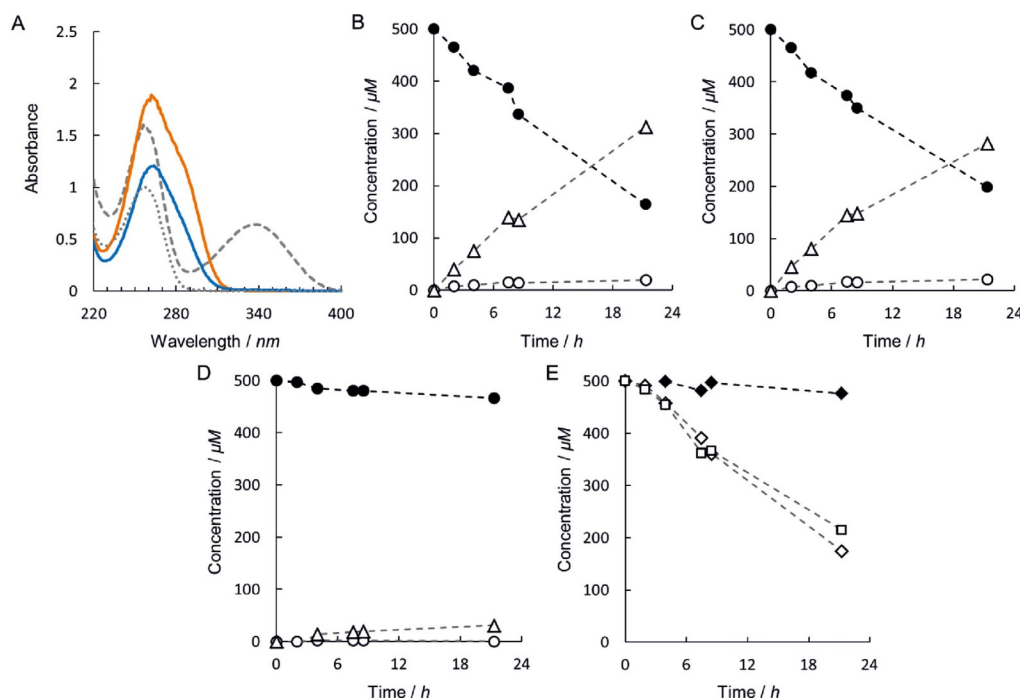


**Figure 2.** Conversion of NADPH catalyzed by ecQueF enzymes and occurring spontaneously in solution. A) The UV/Vis spectra of the main rearrangement product obtained through enzymatic conversion (blue, 80 μM) are compared with the spectra of the cyclization product (orange, 87 μM), NADPH (gray dashed line, 103 μM), and NADP<sup>+</sup> (gray dotted line, 40 μM). B)–E) Time-course analysis of NADPH degradation. Experiments were done in Tris-HCl buffer (100 mM, pH 8.0), additionally containing 50 mM KCl. Enzymatic [B) E89L, C) D197A] and D) spontaneous degradation of NADPH were monitored by HPLC analysis. Closed and open circles indicate NADPH and NADP<sup>+</sup>, respectively. Open triangles indicate NADPH hydration products. E) Degradation of NADPH [spontaneous (◆), E89L (◇), D197A (□)] monitored by loss of absorbance at 340 nm. Reaction rates obtained from the time courses are summarized in Table 2.

The UV/Vis spectra of hydrated and cyclized product differ in a small “hump” in the region of 280–300 nm that the spectrum of the cyclic product characteristically shows.<sup>[16,25]</sup> As shown in Figure 2A, this hump was absent from the spectrum of the enzymatically formed product. The <sup>1</sup>H NMR spectrum of the main product obtained from complete conversion of NADPH in the presence of the D197A variant is depicted in Figure 3B. Comparison of the product spectrum with the <sup>1</sup>H NMR spectrum of NADPH reveals complete disappearance of signals from the dihydronicotinamide C4 protons of NADPH in the product. Moreover, proton signals diagnostic of the cyclized product, namely those from the tetrahydronicotinamide C5 and the ribosyl C1, were not present in the spectrum of the enzymatically formed product (Figure 3B). Therefore, the actual product of the enzymatic conversion is the NADPH hydrate. Its further rearrangement into the cyclized product most likely occurs spontaneously, particularly during sample preparation for, and in, analysis by LC-MS. We also note that a simple *N*-glycosylase-like degradation of NADPH into adenine (mass = 135) and nicotinamide dinucleotide phosphate (mass = 612), previously considered for *Vibrio cholerae* QueF (vcQueF) on the basis of the observation of the 623 mass fragment in the protein crystal,<sup>[11]</sup> is ruled out by these data.

### Time-course analysis of NADPH hydration

The rate of non-enzymatic hydration of NADPH is strongly dependent on the proton concentration.<sup>[25,39]</sup> We therefore

searched for pH conditions (pH 7.5–9.5) that would provide minimum non-enzymatic background for the enzyme-catalyzed hydrations of NADPH. In the same manner, reducing agents were excluded from the reaction. Because of loss of enzyme activity at high pH, the highest usable pH was 8.0. Time courses of enzymatic and spontaneous conversions of NADPH at pH 8.0 are shown in Figure 2B–E. The rates obtained from the data are summarized in Table 2. The kinetics of the formation of NADPH degradation products and of NADP<sup>+</sup> (Figure 2B–D) suggested that hydration and oxidation represented two parallel pathways of NADPH conversion. In the spontaneous conversion, the rate of formation of NADP<sup>+</sup> was decreased up to 60-fold at pH 8.0, relative to pH 7.5, in the presence of DTT (Table 1). (Note: unlike DTT, TCEP can play a catalytic role in the hydration of NADPH.<sup>[18]</sup> comparison of NADPH degradation rates at pH 8.0 and pH 7.5 was therefore considered less meaningful when TCEP was added.) The enzyme-promoted conversion of NADPH in the presence of DTT showed negligible difference in the NADP<sup>+</sup> formation rate at pH 8.0 and at pH 7.5. The conversion of NADPH into NADPHX was decreased only by a factor of up to two as a result of the pH change from 7.5 to 8.0 and it thus remained the main pathway of NADPH degradation. The hydration of NADPH was about 16 times faster than the oxidation of NADPH at pH 8.0. These results strongly support the idea that ecQueF enzymes provide catalytic facilitation to the hydration of the C5=C6 double bond in the dihydronicotinamide moiety of NADPH, thus forming NADPHX. The NADPH conversion detectable by HPLC (Fig-



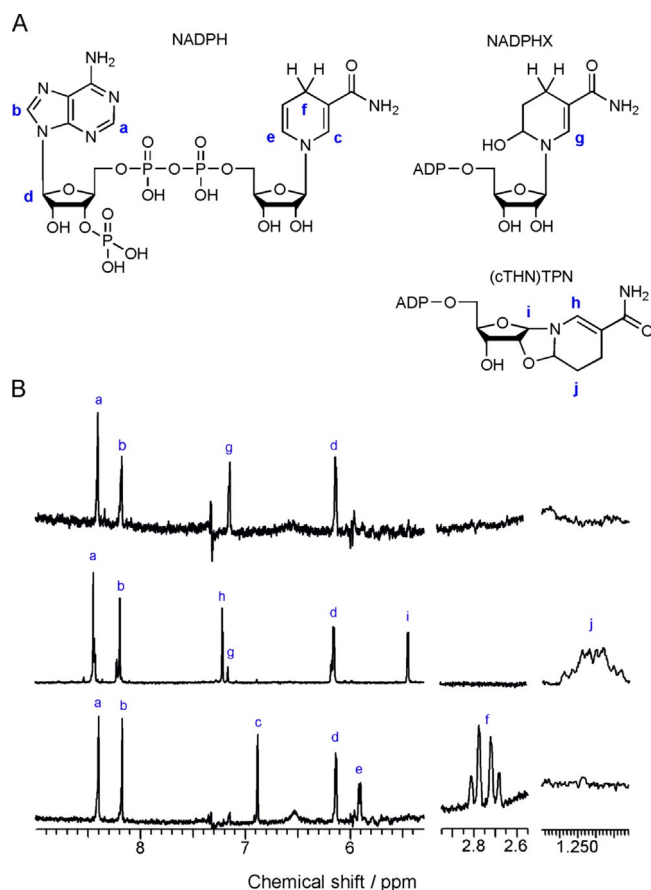


**Figure 3.**  $^1\text{H}$  NMR analysis of the main hydration product released during conversion of NADPH in the presence of the D197A variant of ecQueF. A) Chemical structures involved in NADPH degradation. B) The  $^1\text{H}$  NMR spectrum (top) of the product obtained from full conversion of NADPH (0.5 mM) in the presence of the enzyme (50  $\mu\text{M}$ ). Reference spectra of the cyclic product (middle, 5.8 mM) and of NADPH (bottom, 0.5 mM) are also shown. Tris-HCl buffer (100 mM, pH 7.5) containing 50 mM KCl and 1.15 mM TCEP was used for the reaction. Ribosyl protons overlapped with the water signal. The spectra of NADPH<sup>[38]</sup> and the degradation products<sup>[16,18]</sup> were validated with previously reported spectra of these components.

**Table 2.** Reaction rates at pH 8.0 associated with NADPH degradation in the presence of wild-type ecQueF and variants thereof. The rates are expressed in terms of product released (or substrate converted). Reactions were carried out in Tris buffer (100 mM, pH 8.0; 50 mM KCl) and used 500  $\mu\text{M}$  NADPH. The standard deviations shown are from triplicate measurements.

	NADPH	Reaction rate [ $\mu\text{mol L}^{-1} \text{min}^{-1}$ ]		
		NADP <sup>+</sup>	NADPHX <sup>[a]</sup>	A340 <sup>[c]</sup>
no enzyme	0.039 $\pm$ 0.003	0.0006 $\pm$ 0.0001	0.021 $\pm$ 0.005	0.022 $\pm$ 0.002
D197A <sup>[b]</sup>	0.245 $\pm$ 0.004	0.014 $\pm$ 0.001	0.220 $\pm$ 0.010	0.238 $\pm$ 0.021
E89L <sup>[b]</sup>	0.272 $\pm$ 0.013	0.015 $\pm$ 0.003	0.246 $\pm$ 0.010	0.273 $\pm$ 0.020
C190A/ D197A <sup>[b]</sup>	0.022 $\pm$ 0.001	0.003 $\pm$ 0.0003	0.015 $\pm$ 0.001	0.018 $\pm$ 0.002
E89L/D197A <sup>[b]</sup>	0.042 $\pm$ 0.006	0.010 $\pm$ 0.002	0.047 $\pm$ 0.004	0.057 $\pm$ 0.005
E89Q/ D197A <sup>[b]</sup>	0.030 $\pm$ 0.003	0.012 $\pm$ 0.002	0.017 $\pm$ 0.003	0.029 $\pm$ 0.003

[a] Calculated from the product peak area (Figure 1). [b] The enzyme concentration used was 50  $\mu\text{M}$ . [c] Rates determined from the decrease in absorbance at 340 nm, as shown in Figure 2E.

ure 2B–D) coincided with loss of absorbance at 340 nm, as shown in Figure 2E and Table 2.

### NADH and 1-substituted 1,4-dihyronicotinamides as substrates of hydration

To examine the substrate specificity of the enzymatic hydration, we used the D197A variant of ecQueF. By incubating NADH (500  $\mu\text{M}$ ) in the presence of 50  $\mu\text{M}$  enzyme in air-saturated buffer (100 mM Tris, 50 mM KCl, pH 8.0) we showed that oxidation to NAD<sup>+</sup> ( $63.9 \times 10^{-3} \mu\text{M min}^{-1}$ ) was the main reaction pathway. Hydration of NADH was also observed but at a rate about 10 times slower ( $6.4 \times 10^{-3} \mu\text{M min}^{-1}$ ). In the spontaneous reaction, in contrast, the conversion of NADH to NADHX ( $4.8 \times 10^{-3} \mu\text{M min}^{-1}$ ) was ten times faster than the conversion to NAD<sup>+</sup> ( $0.5 \times 10^{-3} \mu\text{M min}^{-1}$ ). The rate of spontaneous oxidation of NADH to NAD<sup>+</sup> is consistent with the corresponding oxidation rate of NADPH to NADP<sup>+</sup> (Table 2). However, the formation of NADHX was 4.4 times slower than the formation of NADPHX ( $21 \times 10^{-3} \mu\text{M min}^{-1}$ , Table 2). These results show that NADH is not accepted as a substrate for hydration by the D197A variant. Strict specificity for NADPH in the natural reaction with preQ<sub>0</sub><sup>[1]</sup> is thus also reflected in the hydration side reaction.

We then examined enzymatic reactivity with 1-methyl- and 1-benzyl-1,4-dihyronicotinamide. Reactions were monitored by UV/Vis spectrophotometry. As expected, 1-methyl- and 1-benzyl-1,4-dihyronicotinamide show absorbance bands with maximum absorption at 360 nm (Figure S2). Their corresponding hydration products are detectable similarly to NAD(P)HX, through increased absorption at 280–290 nm and complete loss of absorption at 360 nm (Figures S2 and S3). The 1,4-dihyronicotinamides and their corresponding hydrated products were also confirmed by LC-MS (Figure S3). In both enzymatic and spontaneous reactions, we observed conversion to the hydrated products (Figure S4). The hydration rates were not accelerated in the presence of enzyme (Figure S4). In an effort to facilitate binding of the 1,4-dihyronicotinamides to the enzyme, we considered an approach of “substrate in pieces”<sup>[40,41]</sup> and additionally added ADP (1.11 mM). However, the hydration rate in the presence of D197A variant was not affected by ADP (Figure S4).

### Stereospecificity of the enzymatic hydration of NADPH

Spontaneous (acid-catalyzed) hydration of NAD(P)H yields (*R*)- and (*S*)-NAD(P)HX in a ratio of 35:65, as shown in the literature<sup>[18,25,29–31]</sup> and confirmed for the specific reaction conditions used here (Figure 4). GAPDH was shown to produce 60% (*S*)-NADHX and 40% (*R*)-NADHX.<sup>[18]</sup> The cyclized NADPHX epimers were also observed as products of acid-modified NADPH.<sup>[16,29]</sup> The *R*-configured cyclized product was strongly preferred (Figure 4A). Stereochemical preference in the cyclization is explicable in terms of a different—*S<sub>N</sub>2* versus *S<sub>N</sub>1*—character of the nucleophilic substitution at the tetrahyronicotinamide C6 by the ribosyl O2 when epimerized (*S*)-NADPHX or (*R*)-NADPHX, respectively, undergoes cyclization.<sup>[16]</sup>

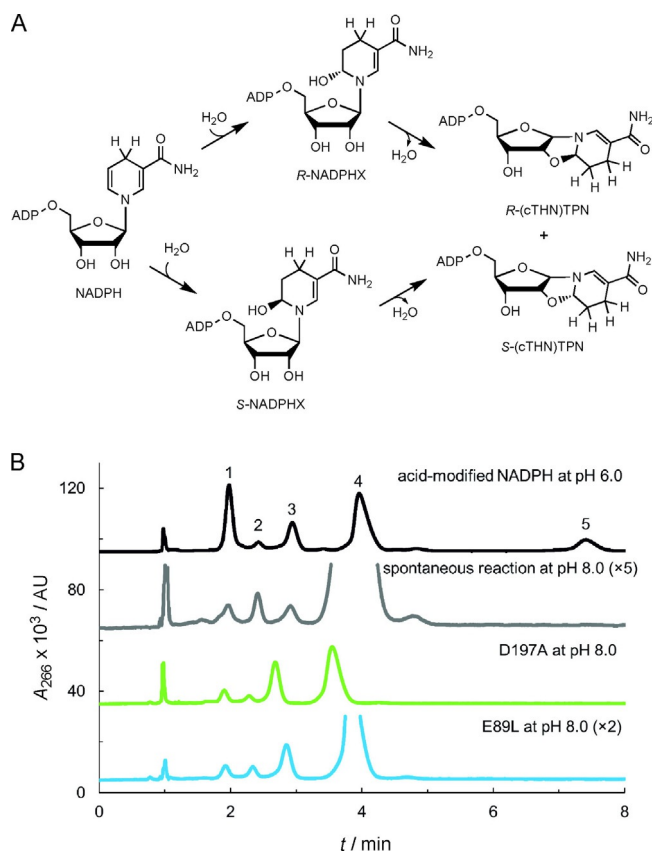


**Figure 4.** Analysis of stereospecificity in the hydration of NADPH in enzyme-promoted and spontaneous reactions. A) NADPH hydration to (*R*)- and (*S*)-NADPHX and further cyclization of the hydrated products. B) HPLC analysis of the products of NADPH hydration. The acid-modified NADPH was prepared at pH 6.0 as described in ref. [30]. Peaks 1 and 3 indicate (*S*)- and (*R*)-NADPHX, respectively. Peaks 2 and 4 indicate NADP<sup>+</sup> and NADPH, respectively. Peak 5 indicates the *R* form of cyclized NADPHX [(cTHN)TPN] as the major stereoisomer. The ratio of *R* and *S* forms was calculated by using peak areas.

Analysis of the stereoselectivity of the enzymatic hydration of NADPH must consider the relatively fast spontaneous epimerization of the hydrated NADPH. Study of NADHX epimerase has revealed that the individual *R* and *S* epimers of NADPH hydrate interconvert readily to a 2:3 equilibrium of the *R* and *S* forms.<sup>[31]</sup> We show here that NADPH solution at pH 8.0 initially contained a small amount of NADPHX consisting of 56% *R* and 44% *S* form (Figure S5 A). The initial *R/S* mixture was converted within about 2.5 h to the expected equilibrium composition. To minimize the effect of spontaneous epimerization in the ecQueF-promoted hydration of NADPH, we analyzed samples from enzymatic reactions after 30 min incubation time. The enzymatic reaction was stopped by rapid filtering-off of the enzyme ( $\leq 15$  min). In addition, the enzymatic reaction was performed at pH 8.0 whereas the analysis was done at pH 7.0. The results are shown in Figure 4B. Using the D197A and the E89L variant in three independent experiments, we showed that the released NADPHX consisted of 78( $\pm 9$ )% (D197A) and 78( $\pm 7$ )% (E89L) *R* form. We analyzed the deproteinized samples again after incubation at 25 °C for 2 h. We showed that a small portion ( $\leq 10\%$ ) of (*R*)-NADPHX had been converted into

the *S* form under these conditions (Figure S5 B). These results demonstrate a certain degree of *R* stereoselectivity in NADPH hydration in the presence of the D197A and E89L variants of ecQueF.

### Enzymatic hydration of NADPH in the presence of double variants of ecQueF

To examine the involvement of ecQueF active-site residues in the hydration of NADPH, we constructed enzyme double variants based on the D197A single variant. The aggregated structural evidence relating to QueF enzymes, including the structural model of the ecQueF-NADPH-preQ<sub>0</sub> complex,<sup>[42]</sup> suggests that Cys190 and Glu89 are positioned close to the nicotinamide moiety of NADPH (Figure 5 A). We substituted Cys190 with an alanine residue to remove a possible general acid catalytic function of the thiol side chain of the cysteine residue (protonation of the dihydronicotinamide C5). We substituted Glu89 with a glutamine residue to remove a possible general base catalytic function in the attack of water on the dihydronicotinamide C6 atom. We additionally replaced Glu89 with a leucine residue to remove coordination to the structural water, close to the reactive C6 atom of NADPH identified in the structure model (Figure 5 A).

The double variants (C190A/D197A, E89L/D197A, and E89Q/D197A) were isolated and incubated with NADPH at pH 8.0. Results are summarized in Table 2. The rate of NADPH hydration in the presence of the C190A/D197A double variant was very low, comparable with that of the spontaneous reaction. Evidence that substitution of Cys190 with alanine effectively disrupts the NADPH hydratase activity in the wild-type enzyme (single C190A variant, Table 1) and in the more active D197A variant (double C190A/D197A variant) supports the contention that Cys190 is essential for NADPH hydration. The double variants incorporating substitutions of Glu89 showed very low activity (Table 2). NADPH hydration in the presence of the E89L/D197A variant proceeded about twice as rapidly as the spontaneous hydration. The E89Q/D197A variant did not accelerate NADPHX formation above the non-enzymatic rate. The single-site substitutions E89L and D197A appear to be antagonistic, or are not mutually compatible with one another, with regard to the NADPH hydration activity.

### Proposed mechanism of NADPH hydration through the action of ecQueF

Spontaneous conversion of NAD(P)H to the cyclized product via the hydrated intermediate (Scheme 2)<sup>[16,18,24]</sup> is accelerated strongly in the presence of polybasic anions (e.g., pyrophosphate, phosphate, citrate). The conversion of NADH through the action of GAPDH is likewise accelerated by polybasic anions.<sup>[18]</sup> Like ecQueF, GAPDH uses an active-site cysteine residue as catalytic nucleophile of the reaction.<sup>[18,27,28]</sup> NADH was hydrated more rapidly in the presence of GAPDH with the relevant cysteine acylated than in that of the corresponding apoenzyme. It was suggested that hydration of the C5=C6 double bond occurs from a ternary complex between acylated

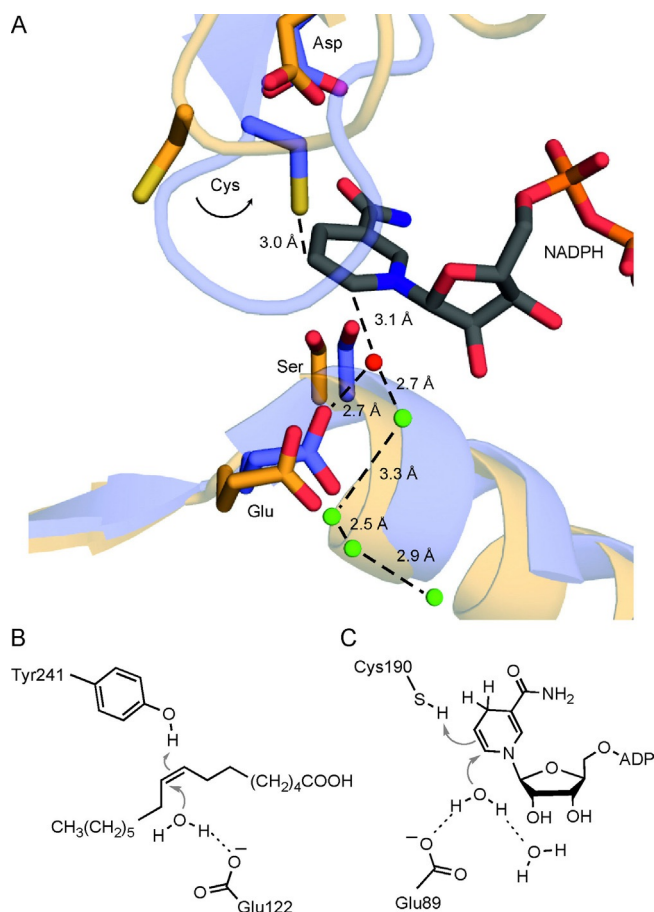


**Figure 5.** A) Structural interpretation of catalytic hydration of NADPH by the D197A variant of ecQueF, and possible mechanistic analogy with B) oleic hydratase, and C) ecQueF in carbon–carbon double bond hydration. A) Overlay of the structural model of ecQueF<sup>[42]</sup> (orange, wild-type enzyme) and the experimentally determined crystal structure of *V. cholerae* QueF (light blue, R262L variant, PDB ID: 3UXJ). The bound NADPH is from the structural model of ecQueF. The catalytic Cys residue is on a flexible loop in the QueF structures. Amino acids and NADPH are indicated by element-based colors. Water molecules are shown as red and green spheres. B) The proposed catalytic mechanism of substrate hydration through the action of the oleic hydratase from *E. meningoseptica*,<sup>[43,44]</sup> and C) the tentative mechanism of NADPH hydration through the action of the D197A variant of ecQueF. In both cases a catalytic acid moiety manages proton transfer to carbon. Stereospecific attack of water can be facilitated by a Glu residue that functions as a catalytic base.

enzyme, NADH, and polybasic anion.<sup>[18]</sup> The acylated GAPDH was shown to bind to NADH more tightly than to NAD<sup>+</sup>.<sup>[27,28]</sup>

Although degradation of NADPH in the presence of ecQueF (e.g., D197A and E89L variants) involves the same hydration event on the dihydronicotinamide moiety as the conversion of NADH by GAPDH does, the underlying mechanisms are clearly different. The activity of ecQueF does not rely on modification of the active-site cysteine residue. It is not dependent on the presence of polybasic anions and proceeds readily in their absence at pH 7.5–8.0. Mutagenesis results suggest the essential involvement of Cys190 in the degradation of NADPH in the presence of ecQueF. Unlike the Asp197 single variants and also the wild-type enzyme, the C190A and C190S variants do not show NADPH hydration activity above the background of the

control. In view of the position of Cys190 relative to the reactive nicotinamide C5 atom in NADPH, which appears suitable for proton transfer (Figure 5A), we would like to suggest a role for the cysteine residue as catalytic acid in the C5=C6 double bond hydration through the action of the enzyme. Indeed, the hydration activity was eliminated in the case of C190A/D197A double variant (Table 2), thus strongly supporting the proposed role of Cys190 in enzymatic hydration of NADPH.

The effect of site-directed substitution of Asp197 by Ala in enhancing the enzymatic hydration rate is thus explainable in a twofold manner. Firstly, the substitution will enhance the conformational flexibility of Cys190, as indicated in Figure 5A, and this might be important for the cysteine residue's proper function as proton donor. Secondly, it will probably stabilize Cys190 in a reactive (protonated) state because the Asp residue responsible for deprotonation of the cysteine residue in the normal catalytic reaction (Scheme 1) is replaced by a residue incapable of fulfilling an analogous function. The enzyme structures (Figure 5A) also indicate that a water molecule is in a position potentially suitable for attack on the reactive C6 atom of NADPH. However, from its position at the side of the nicotinamide ring, the water is not placed well for stereospecific attack on nicotinamide carbon atom 6. To give the *R*-configured NADPHX product, the water would have to react from below the nicotinamide ring. However, the potentially relevant water is connected to Glu89 and is part of a chain of water molecules leading from the enzyme active site to bulk solvent (Figure 5). Formation of the *R*-configured product is preferred over that of the *S*-configured product by a factor of 3.5. The enzyme structure model (Figure 5A) suggests that addition of water might be facilitated by Glu89 providing some base catalytic assistance. However, the mutagenesis results (E89L variant) do not support direct involvement of Glu89 in the catalytic hydration.

The evidence that substitutions E89L and D197A, which are effective in single enzyme variants in eliciting hydratase activity, cannot be combined in an active double variant of the enzyme (E89L/D197A) suggests that relative positioning of the Cys190 and the dihydronicotinamide C5 atom for proton transfer requires a subtle balance of structural factors. Tentatively, the D197A substitution can enhance the conformational flexibility of Cys190. The E89L substitution, in contrast, can cause minor change in the binding of the NADPH nicotinamide moiety. Each individual effect could plausibly be conducive to the hydration of NADPH but the combination of the two might not be beneficial.

The proposed pathway of NADPH hydration in the presence of ecQueF bears some mechanistic resemblance to C=C double bond hydration in the presence of cofactor-independent hydratases, such as fatty acid (de)hydratases, linalool dehydratase-isomerases and carotenoid hydratases.<sup>[43,45,46]</sup> These hydratases have attracted considerable attention in view of their potential use in biocatalytic synthesis through regio- and stereoselective hydration reactions.<sup>[44,45,47,48]</sup> Mechanistically, as shown in the case of the oleic hydratase from *Elizabethkingia meningoseptica*,<sup>[43,44,46]</sup> C=C double bond hydration proceeds according to a concerted general acid- and general base-cata-



lyzed reaction process. Specifically, a tyrosine residue (Tyr241) is responsible for proton transfer to carbon and the stereospecific attack of water is facilitated by a glutamate residue (Glu122, Figure 5B). The possible mechanistic analogy between ecQueF and natural hydratases is thus immediately recognizable from Figure 5B and C.

## Conclusion

The *E. coli* nitrile reductase was discovered to catalyze the slow hydration of NADPH ( $k_{\text{cat}} \approx 10^{-2} \text{ min}^{-1}$  in the most active D197A and E89L variants). The enzymatic reaction, which to the best of our knowledge is reported here for the first time, was shown to consist of the protonation of the C5 atom and the addition of water to the C6 atom of the dihydronicotinamide moiety of NADPH. The addition of water proceeds with some degree of stereocontrol (78% *R*) by the enzyme. The hydrated NADPH undergoes spontaneous cyclization. The proposed enzymatic mechanism of NADPH hydration involves Cys190 as the general catalytic acid for protonation of the dihydronicotinamide C5 atom. It is suggested that the effects of site-directed replacements of Asp197 (D197A) and Glu89 (E89L) on enhancement of the hydratase activity arise from increased conformational flexibility of Cys190 (D197A) and slight repositioning of the dihydronicotinamide ring in the active site (E89L). Mechanistically, the proposed reaction of the nitrile reductase shows analogy with the catalytic addition of water to carbon-carbon double bond through the action of natural hydratases.

## Experimental Section

**Chemicals:** NAD(P)H (purity >98%) and NAD(P)<sup>+</sup> (purity >97%) were from Carl Roth (Karlsruhe, Germany). Materials were of the highest purity available from Carl Roth and Sigma-Aldrich. The preQ<sub>0</sub> was synthesized as described previously.<sup>[49]</sup> 1-Benzyl-1,4-dihydronicotinamide was from TCI Deutschland, GmbH (Eschborn, Germany). 1-Methyl-1,4-dihydronicotinamide was from Toronto Research Chemicals (North York, ON, Canada).

**Site-directed mutagenesis and enzyme preparation:** Mutagenesis to substitute Glu89 with Leu (E89L), Cys190 with Ala (C190A) and Ser (C190S), and Asp197 with Ala (D197A) or His (D197H) was reported in earlier studies of ecQueF.<sup>[10,12,42]</sup> Genes encoding the double variants (C190A/D197A, E89L/D197A, E89Q/D197A) were obtained from Genscript (Piscataway, NJ, USA). All mutations were verified by gene sequencing. The ecQueF variants were obtained as N-terminally His-tagged proteins through expression in *E. coli* BL21-DE3 as described previously.<sup>[9,10]</sup> All enzymes were purified by use of a reported two-step procedure consisting of immobilized metal ion affinity chromatography and gel filtration.<sup>[9,10]</sup> Enzyme purity was confirmed by SDS-PAGE. The HisTrap affinity column (GE Healthcare, Buckinghamshire, UK) was regenerated fully after each use. The PD10-desalting columns (GE Healthcare) were always freshly used. Contamination with protein carried over from previous purification runs was thus rigorously ruled out. Protein concentration was measured with a Pierce BCA protein assay kit (Thermo Fisher Scientific). Enzyme stock solutions (0.4–0.8 mM) were stored at –20 °C and used within three weeks.

**Enzymatic activity of ecQueF variants toward preQ<sub>0</sub> reduction:** Reactions for preQ<sub>0</sub> reduction were carried out at 25 °C with agitation at 500 rpm in a Thermomixer Comfort instrument (Eppendorf, Hamburg, Germany). The enzyme solutions of ecQueF wild type (5 μM) and variants thereof (50 μM) were prepared in Tris-HCl buffer (pH 7.5, 100 mM), additionally containing KCl (50 mM) and TCEP (1.15 mM). The preQ<sub>0</sub> and NADPH concentrations were 250 and 500 μM, respectively. The reaction volume was 1–1.5 mL. Samples were taken at certain times up to 96 h. Enzyme was removed by precipitation with methanol (10%, by volume) at 70 °C for 10 min (agitation at 1000 rpm). The product solutions were analyzed by HPLC with UV/Vis and/or MS detection. All compounds known to be involved in the reaction according to Scheme 1 (preQ<sub>0</sub>, preQ<sub>1</sub>, NADPH, NADP<sup>+</sup>) were analyzed, as shown in Figure S1. In addition, degradation products of NADPH were revealed (Figure S1). Data were obtained from triplicate experiments.

**Enzymatic activity of ecQueF variants toward NADPH degradation:** The enzyme solution (50 μM) was incubated in the presence of NADPH (500 μM). Tris-HCl buffer (pH 7.5, 100 mM) containing KCl (50 mM) was prepared with either TCEP or DTT (1.15 mM). Alternatively, the same Tris-HCl buffer was prepared at pH 8.0 without TCEP or DTT. Enzyme solution was gel-filtered twice to the used buffer before the reaction was started. The reaction volume was 1–1.5 mL. After incubation at 25 °C for up to 26 h (600 rpm, Thermomixer Comfort), the reaction was stopped by precipitating the enzyme with twice the reaction volume of acetonitrile (15 min on ice). Products of enzymatic and spontaneous reactions were analyzed by UV/Vis spectroscopy, HPLC, LC-MS, and <sup>1</sup>H NMR. UV/Vis spectrophotometric analysis was conducted by scanning the products at 220–600 nm with a Beckman DU 800 spectrophotometer (Beckman Coulter, Pasadena, CA, USA). Data were obtained from triplicate experiments.

The “acid-modified” product of NADPH was prepared as described previously.<sup>[25,37]</sup> NADPH solution in water (20.4 mM) was incubated at pH 3.5 (adjusted with 1 M HCl) until more than 95% of the NADPH was consumed. The solution was adjusted to pH 8.2 with NaOH (0.1 M) to prevent further conversion. The product thus obtained is (cTHN)TPN (Scheme 2), as shown by LC-MS and <sup>1</sup>H, <sup>13</sup>C, HSQC, and HMBC NMR analysis.

**<sup>1</sup>H NMR measurements:** NMR spectra were recorded at 499.98 MHz and 30 °C with a Varian INOVA 500 MHz spectrometer (Agilent Technologies) and use of VNMRJ 2.2D software. D<sub>2</sub>O (99.8% D, 20%, v/v) was added to the product solution obtained from enzymatic and spontaneous reaction before the measurements. The (cTHN)TPN obtained from NADPH under acidic conditions was diluted threefold by addition of D<sub>2</sub>O before the measurements. The <sup>1</sup>H and <sup>13</sup>C NMR spectra of coenzymes and of the hydration and the cyclisation product of NADPH were reported previously.<sup>[16,18,37,38,50]</sup> The spectra obtained here were shown to agree well with those earlier spectra.

**HPLC analysis:** The products of NADPH degradation were analyzed at 30 °C with an Agilent 1200 HPLC system (Santa Clara, CA, USA) equipped with a 1.15 μm Cromolith high-resolution RP-18 end-capped column (150 Å, 100×4.6 mm, Merck) and a UV detector (λ = 254, 262, and 340 nm). A gradient (5 to 16%) of acetonitrile in buffer [sodium phosphate (pH 6.8, 50 mM), tetrabutylammonium hydrogensulfate (2 mM)] over 10 min was used. The flow rate was 2 mL min<sup>-1</sup>. The injection volume was 10 μL. The obtained data are shown in Figure S1 and Table S1. Optionally, a Shimadzu LCMS-2020 system (Kyoto, Japan) equipped with a SeQuant ZIC-HILIC column (200 Å, 250×2.1 mm, Merck, Billerica, MA, USA) and the



corresponding guard column (20×2.1 mm, Merck) was utilized to analyze the NADH and NADPH rearrangement products. Note: the method using the Cromolith RP-18 column was incompatible with LC-MS analysis because the sodium phosphate and tetrabutylammonium hydrogensulfate used are not volatile. A linear gradient (80 to 71%) of acetonitrile in buffer [ammonium acetate (pH 6.67 or pH 7.5, 5 mM)] over 12 min was used. The column was washed with acetonitrile (80%) for 6 min. The flow rate was 0.5 mL min<sup>-1</sup>. A UV detector ( $\lambda = 254$  and 340 nm) was used. Masses were scanned over the range of 100–900 with positive and negative mode. The masses of NADH (1 H<sup>+</sup>, 666; 1 H<sup>-</sup>, 664), of NADHX (1 H<sup>-</sup>, 682; 2 H<sup>-</sup>, 340.5), and of NADPHX (1 H<sup>-</sup>, 762; 2 H<sup>-</sup>, 380.5) were also analyzed in SIM mode. The obtained data are shown in Figures 1 and 2 as well as in Tables 1 and 2. Products from enzyme-promoted and spontaneous hydration of the 1,4-dihyronicotinamides were analyzed as described above. A linear gradient of 85 to 73% over 12 min was used. The column was washed with acetonitrile (85%) for 6 min. A UV detector ( $\lambda = 280$ , 290 and 360 nm) was used. The masses of 1-methyl-1,4-dihyronicotinamide (1 H<sup>+</sup>, 139), 1-benzyl-1,4-dihyronicotinamide (1 H<sup>+</sup>, 215), adenosine diphosphate (1 H<sup>+</sup>, 428; 1 H<sup>-</sup>, 426), and the hydrated products (methyl compound, 1 H<sup>+</sup>, 157; benzyl compound, 1 H<sup>+</sup>, 233) were also analyzed in SIM mode. The data are shown in Figures S3 and S4.

**Stereospecificity of NADPH hydration through enzyme-promoted and spontaneous reactions:** The acid-modified products of NADPH were prepared at pH 6.0, as described previously.<sup>[30]</sup> Tris-HCl (100 mM, pH 8.0) additionally containing KCl (50 mM) was used. NADPH (500  $\mu$ M) was added to the enzyme solution (E89L or D197A variant, 200  $\mu$ M). After incubation at 25 °C for 30 min, the enzyme was filtered off rapidly within 15 min. A clear solution was obtained and subjected to HPLC analysis immediately. Rapid handling was used to minimize the effect of spontaneous epimerization of the NADPH hydrate formed in the enzymatic reactions. The epimerization is reported in ref. [31] and we confirmed it here in our own experiments (Figure S5A). The time required for reaction (30 min) and analysis (30 min, including sample preparation) is short enough to prevent substantial interference from spontaneous epimerization (Figure S5B). Note: any addition of acetonitrile to the sample compromises the separation of the hydrated product *R* and *S* forms. A Shimadzu LCMS-2020 system equipped with an EC Nucleodur C<sub>18</sub> gravity column (3.0  $\mu$ m, 150×3 mm, Macheray-Nagel) was used to analyze the products of NADPH hydration. An isocratic flow of ammonium acetate (pH 7.0, 5 mM) was used for 5 min, followed by a linear gradient of up to 5% acetonitrile over 10 min. The column was washed with 90% acetonitrile for 5 min after each analysis. The flow rate was 0.7 mL min<sup>-1</sup>. A UV detector ( $\lambda = 266$  and 340 nm) was used. The data are shown in Figures 4 and S5). Products were identified by those characteristic spectra and comparison with the literature.<sup>[29,30]</sup>

## Acknowledgements

This work has been supported by the COMET Funding Program managed by the Austrian Research Promotion Agency FFG. We thank Prof. Hansjörg Weber (Institute of Organic Chemistry, Graz University of Technology) for <sup>1</sup>H NMR measurements and Dr. Gernot Strohmeier (Austrian Centre of Industrial Biotechnology) for HPLC-MS analysis.

## Conflict of Interest

The authors declare no conflict of interest.

**Keywords:** C=C double bond hydration · cofactors · hydration · NADPH · nitrile reductases

- [1] S. G. Van Lanen, J. S. Reader, M. A. Swairjo, V. de Crécy-Lagard, B. Lee, D. Iwata-Reuyl, *Proc. Natl. Acad. Sci. USA* **2005**, *102*, 4264–4269.
- [2] B. W. K. Lee, S. G. Van Lanen, D. Iwata-Reuyl, *Biochemistry* **2007**, *46*, 12844–12854.
- [3] A. J. M. Ribeiro, L. Yang, M. J. Ramos, P. A. Fernandes, Z.-X. Liang, H. Hirao, *ACS Catal.* **2015**, *5*, 3740–3751.
- [4] D. Iwata-Reuyl, *Bioorg. Chem.* **2003**, *31*, 24–43.
- [5] B. El Yacoubi, M. Bailly, V. de Crécy-Lagard, *Annu. Rev. Genet.* **2012**, *46*, 69–95.
- [6] J. S. Reader, D. Metzgar, P. Schimmel, V. de Crécy-Lagard, *J. Biol. Chem.* **2004**, *279*, 6280–6285.
- [7] M. Vinayak, C. Pathak, *Biosci. Rep.* **2010**, *30*, 135–148.
- [8] V. M. Chikwana, B. Stec, B. W. K. Lee, V. de Crécy-Lagard, D. Iwata-Reuyl, M. A. Swairjo, *J. Biol. Chem.* **2012**, *287*, 30560–30570.
- [9] J. Jung, T. Czabany, B. Wilding, N. Klempier, B. Nidetzky, *J. Biol. Chem.* **2016**, *291*, 25411–25426.
- [10] J. Jung, B. Nidetzky, *J. Biol. Chem.* **2018**, *293*, 3720–3733.
- [11] Y. Kim, M. Zhou, S. Moy, J. Morales, M. A. Cunningham, A. Joachimiak, *J. Mol. Biol.* **2010**, *404*, 127–137.
- [12] J. Jung, J. Braun, T. Czabany, B. Nidetzky, *Catal. Sci. Technol.* **2019**, *9*, 842–853.
- [13] D. Hofmann, A. Wirtz, B. Santiago-Schübel, U. Disko, M. Pohl, *Anal. Bioanal. Chem.* **2010**, *398*, 2803–2811.
- [14] C. Bernofsky, S. Y. Wanda, *J. Biol. Chem.* **1982**, *257*, 6809–6817.
- [15] J. T. Wu, L. H. Wu, J. A. Knight, *Clin. Chem.* **1986**, *32*, 314–319.
- [16] N. J. Oppenheimer, N. O. Kaplan, *Biochemistry* **1974**, *13*, 4675–4685.
- [17] F. Petrat, T. Bramey, M. Kirsch, U. Kerkweg, H. De Groot, *Free Radical Res.* **2006**, *40*, 857–863.
- [18] N. J. Oppenheimer, N. O. Kaplan, *Biochemistry* **1974**, *13*, 4685–4694.
- [19] S. K. Spaans, R. A. Weusthuis, J. van der Oost, S. W. M. Kengen, *Front. Microbiol.* **2015**, *6*, 742.
- [20] C. Nowak, A. Pick, L. I. Csepei, V. Sieber, *ChemBioChem* **2017**, *18*, 1944–1949.
- [21] K. Ortmayr, J. Nocon, B. Gasser, D. Mattanovich, S. Hann, G. Koellensperger, *J. Sep. Sci.* **2014**, *37*, 2185–2191.
- [22] W. Lu, L. Wang, L. Chen, S. Hui, J. D. Rabinowitz, *Antioxid. Redox Signaling* **2018**, *28*, 167–179.
- [23] B. M. Anderson, C. D. Anderson, *J. Biol. Chem.* **1963**, *238*, 1475–1478.
- [24] J. R. Miksic, P. R. Brown, *Biochemistry* **1978**, *17*, 2234–2238.
- [25] A. Yoshida, V. Dave, *Arch. Biochem. Biophys.* **1975**, *169*, 298–303.
- [26] L. Rover Júnior, J. C. Fernandes, G. de Oliveira Neto, L. T. Kubota, E. Katakawa, S. H. Serrano, *Anal. Biochem.* **1998**, *260*, 50–55.
- [27] F. J. Seydoux, N. Kelemen, N. Kellershohn, C. Roucou, *Eur. J. Biochem.* **1976**, *64*, 481–489.
- [28] N. Kelemen, N. Kellershohn, F. Seydoux, *Eur. J. Biochem.* **1975**, *57*, 69–78.
- [29] S. A. Acheson, H. N. Kirkman, R. Wolfenden, *Biochemistry* **1988**, *27*, 7371–7375.
- [30] T. D. Niehaus, L. G. L. Richardson, S. K. Gidda, M. El Badawi-Sidhu, J. K. Meissen, R. T. Mullen, O. Fiehn, A. D. Hanson, *Plant Physiol.* **2014**, *165*, 52–61.
- [31] A. Y. Marbaix, G. Noël, A. M. Detroux, D. Vertommen, E. Van Schaftingen, C. L. Linster, *J. Biol. Chem.* **2011**, *286*, 41246–41252.
- [32] G. T. Bommer, E. Van Schaftingen, M. Veiga-da-Cunha, *Trends Biochem. Sci.* **2019**, <https://dx.doi.org/10.1016/j.tibs.2019.07.004>.
- [33] J. Becker-Ketter, N. Paczia, J. F. Conrotte, C. Zhu, O. Fiehn, P. P. Jung, L. M. Steinmetz, C. L. Linster, *FEBS J.* **2018**, *285*, 3376–3401.
- [34] L. S. Kremer, K. Danhauser, D. Herebian, D. Petkovic Ramadža, D. Piekutowska-Abramczuk, A. Seibt, W. Müller-Felber, T. B. Haack, R. Ploski, K. Lohmeier, D. Schneider, D. Klee, D. Rokicki, E. Mayatepek, T. M. Strom, T.

- Meitinger, T. Klopstock, E. Pronicka, J. A. Mayr, I. Baric, F. Distelmaier, H. Prokisch, *Am. J. Hum. Genet.* **2016**, *99*, 894–902.
- [35] N. J. Van Bergen, Y. Guo, J. Rankin, N. Paczia, J. Becker-Kettern, L. S. Kremer, A. Pyle, J. F. Conrotte, C. Ellaway, P. Procopis, K. Prelog, T. Hamfray, J. Baptista, E. Baple, M. Wakeling, S. Massey, D. P. Kay, A. Shukla, K. M. Girisha, L. E. S. Lewis, S. Santra, R. Power, P. Daubeney, J. Montoya, E. Ruiz-Pesini, R. Kovacs-Nagy, M. Pritsch, U. Ahting, D. R. Thorburn, H. Prokisch, R. W. Taylor, J. Christodoulou, C. L. Linster, S. Ellard, H. Hakonarson, *Brain* **2019**, *142*, 50–58.
- [36] P. Prabhakar, J. I. Laboy, J. Wang, T. Budker, Z. Z. Din, M. Chobanian, L. A. Fahien, *Arch. Biochem. Biophys.* **1998**, *360*, 195–205.
- [37] N. J. Oppenheimer, *Biochem. Biophys. Res. Commun.* **1973**, *50*, 683–690.
- [38] E. Ragg, L. Scaglioni, R. Mondelli, I. Carelli, A. Casini, S. Tortorella, *Biochim. Biophys. Acta* **1991**, *1076*, 49–60.
- [39] G. W. Rafter, S. Chaykin, E. G. Krebs, *J. Biol. Chem.* **1954**, *208*, 799–811.
- [40] S. A. Kholodar, C. L. Allen, A. M. Gulick, A. S. Murkin, *J. Am. Chem. Soc.* **2015**, *137*, 2748–2756.
- [41] J. P. Richard, *J. Am. Chem. Soc.* **2019**, *141*, 3320–3331.
- [42] B. Wilding, M. Winkler, B. Petschacher, R. Kratzer, S. Egger, G. Steinkellner, A. Lyskowski, B. Nidetzky, K. Gruber, N. Klempier, *Chem. Eur. J.* **2013**, *19*, 7007–7012.
- [43] M. Engleder, T. Pavkov-Keller, A. Emmerstorfer, A. Hromic, S. Schrempf, G. Steinkellner, T. Wriessnegger, E. Leitner, G. A. Strohmeier, I. Kaluzna, D. Mink, M. Schürmann, S. Wallner, P. Macheroux, K. Gruber, H. Pichler, *ChemBioChem* **2015**, *16*, 1730–1734.
- [44] R. M. Demming, S. C. Hammer, B. M. Nestl, S. Gergel, S. Fademrecht, J. Pleiss, B. Hauer, *Angew. Chem. Int. Ed.* **2019**, *58*, 173–177; *Angew. Chem.* **2019**, *131*, 179–183.
- [45] M. Engleder, H. Pichler, *Appl. Microbiol. Biotechnol.* **2018**, *102*, 5841–5858.
- [46] R. M. Demming, M.-P. Fischer, J. Schmid, B. Hauer, *Curr. Opin. Chem. Biol.* **2018**, *43*, 43–50.
- [47] M. Engleder, G. A. Strohmeier, H. Weber, G. Steinkellner, E. Leitner, M. Müller, D. Mink, M. Schürmann, K. Gruber, H. Pichler, *Angew. Chem. Int. Ed.* **2019**, *58*, 7480–7484; *Angew. Chem.* **2019**, *131*, 7558–7563.
- [48] B. S. Chen, L. G. Otten, U. Hanefeld, *Biotechnol. Adv.* **2015**, *33*, 526–546.
- [49] B. Wilding, M. Winkler, B. Petschacher, R. Kratzer, A. Glieder, N. Klempier, *Adv. Synth. Catal.* **2012**, *354*, 2191–2198.
- [50] T. J. Williams, A. P. Zens, J. C. Wisowaty, R. R. Fisher, R. B. Dunlap, T. A. Bryson, P. D. Ellis, *Arch. Biochem. Biophys.* **1976**, *172*, 490–501.

---

Manuscript received: November 6, 2019

Accepted manuscript online: December 18, 2019

Version of record online: February 20, 2020